Konrad-Zuse-Zentrum für Informationstechnik Berlin

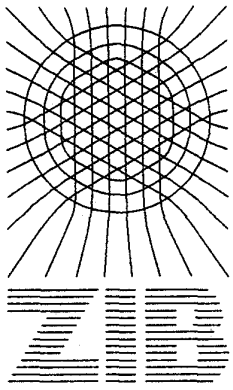

ANDREAS HOHMANN

An Adaptive Continuation Method for Implicitly Defined Surfaces

Preprint SC 91-20 (December 1991)

Herausgegeben vom
Konrad-Zuse-Zentrum für Informationstechnik Berlin
Heilbronner Str. 10
1000 Berlin 31
Verantwortlich: Dr. Klaus André
Umschlagsatz und Druck: Rabe KG Buch-und Offsetdruck Berlin

ISSN 0933-7911

An Adaptive Continuation Method for Implicitly Defined Surfaces

ANDREAS HOHMANN

Konrad–Zuse–Zentrum für Informationstechnik Berlin, Heilbronner Strasse 10, D-1000 Berlin 31, Federal Republic of Germany

December 20, 1991

ABSTRACT

A new method for the numerical aproximation of an implicitly defined surface is presented. It is a generalization of the Euler-Gauss-Newton method for implicitly defined (one-parameter) curves to the case of (two-parameter) surfaces. The basic task in the more general case is an efficient combination of modern CAGD techniques (such as triangular Bernstein-Bézier patches and the nine parameter Hermite interpolant) and the rank deficient Gauss-Newton method.

Contents

INTRODUCTION

Consider a finite dimensional dynamical system $\dot{x} = f(x, \lambda)$ depending on k scalar parameters. Its steady state solutions form under suitable conditions a k dimensional smooth manifold M in some n-dimensional Euclidian space being the zero set of the underlying parameter-dependent vector field. Thus, the investigation of parameter-dependent systems leads to implicitly defined smooth manifolds, i.e. the zero sets of differtiable mappings from some open subset $D \subset \mathbf{R}^n$ in $\mathbf{R}^m = \mathbf{R}^{n-k}$ having 0 as a regular value.

In this paper we only treat the case $k = 2$, i.e. M is an implicitly defined surface in $\mathbf{R}^n$. We are concerned with the numerical approximation of M or more precisely of the connected component of M containing a given initial solution $y_0 \in M$. In the one-dimensional case, where M is an implicitly defined curve, the problem is quite well understood and there are effective algorithms at hand. The numerical methods may be devided into two groups: *continuation* methods (also called *homotopy* or *predictor-corrector* methods) and *piecewise linear* (short PL-) methods. Of the first category are the methods by Rheinboldt [14], Deuflhard, Fiedler and Kunkel [12], Keller [11], Doedel [7] or Seydel [16]. For an extensive survey, also of the second category, we refer to Allgower and Georg [1]. They are all restricted to the case $k = 1$ of implicitly defined curves having no canonical generalization for manifolds of higher dimension. Rheinboldt [15] has shown that it is possible to save the continuation idea for $k > 1$ by "projecting" a fixed triangulation of the tangent space at a point onto the manifold, where "projecting" means a Gauss Newton process. Of course this can only be done locally, i.e., as long as a so-called *moving frame* exists and the triangulation of the tangent space is suitable for the manifold. In addition, it seems to be very difficult to achieve adaptivity comparable with the steplength control mechanisms being standard for continuation methods in one parameter.

In contrast to continuation methods, the piecewise linear methods do not know the principal barrier $k = 1$. A first algorithm for the piecewise linear approximation of an implicitly defined manifold for arbitrary k was published by Allgower and Schmidt [4]. It was further developed by Gnutzmann [2] [3], who in paricular implemented the method for surfaces ($k = 2$) showing its reliability for small n. A similar method was developed by Bloomenthal [5] who is mainly interested in CAGD applications and therefore only considers surfaces in the three dimensional Euclidian space.

These two methods show a principal disadvantage of PL methods. Using n-simplices which are successively refined to approximate the given manifold, the piecewise linear approach is rather complicated and extremely costly for

large dimensions n of the underlying space. Since we definitely aim at tackling problems in higher dimensional spaces, we are looking for a method that shares the advantages with the one-parameter continuation approach like adaptivity and effectivity for large n but is not refined to the local approximation of a given manifold.

In this paper we show that it is in fact possible to approximate an implicitly defined surface ($k = 2$) globally using a locally adaptive continuation process. We construct a triangulation and at the same time a continuous cubic approximation of the surface by successively computing new points on the surface and fitting the resulting triangles together. The main ingredients of the method are

- a Gauss Newton method (with rank deficiency k) as corrector scheme
- the nine parameter Hermite interpolant as a local approximation and predictor scheme
- elementary geometrical considerations to connect the triangles.

We begin in Section 1 with a rough description of the algorithm. In Sections 2 to 4 we derive the necessary theoretical concepts. Section 5 is devoted to the realization of the method and in Section 6 we give some simple but instructive numerical examples.

1 A TWO-DIMENSIONAL CONTINUATION ALGORITHM

In this section we sketch the main ideas of the two-dimensional continuation method leaving some notions and details for further explanation in the following sections. Let $f : D \subset \mathbf{R}^n \to \mathbf{R}^m$, $n = m + 2$, be a twice differentiable mapping of some open subset $D \subset \mathbf{R}^n$ in $\mathbf{R}^m$ such that $0 \in \mathbf{R}^m$ ist a regular value of f, i.e. the Jacobian $f'(y)$ has full rank at all solutions $y \in D$ of $f(y) = 0$. Under these conditions the solutions form a k dimensional submanifold

$$M := \{y \in D \mid f(y) = 0\} \tag{1.1}$$

of $\mathbf{R}^n$. Moreover, suppose that an initial approximate solution $\hat{y}_0 \in D$ of $f(y) = 0$ is given.

To generate the connected component of M containing a solution $y_0 \in M$ near $\hat{y}_0$ the first step is to compute an initial triangle on M. After a first single solution $y_0 \in M$ has been obtained by a rank deficient Gauss-Newton method applied to $\hat{y}_0$, we employ a tangent continuation method in two linear independent directions t_i on the tangent plane at y_0 to get two further solutions $y_1, y_2 \in M$. We thus construct a triangle $T = \{y_0, y_1, y_2\} \subset M$ on M which constitutes our initial triangulation $\mathcal{T} = \{T\}$.

For each free edge of the triangulation, i.e. belonging to a single triangle, we now construct an extrapolated (imaginary) triangle using the data of the corresponding triangle and the convergence properties of the Gauss-Newton process for its vertices.

In a next step we try to realize these extrapolated triangle by either connecting them directly to appropriate already existing triangles or by computing a new solution on M. In the latter case we create two new edges to continue the process with.

Describing the algorithm in a more detailed fashion, we proceed as follows:

ALGORITHM 1.

- Compute a first solution $y_0 \in M$ by means of an Gauss Newton iteration $\hat{y}_0 \overset{GN}{\longmapsto} y_0$ with starting point $y^0 = \hat{y}_0$ (see section 2).

- Compute two further solutions $y_1, y_2 \in M$ using a tangent continuation method

$$y_0 + s_i t_i \overset{GN}{\longmapsto} y_i \quad \text{for } i = 1, 2,$$

where $t_1, t_2 \in T_{y_0}M = \ker Df(y_0)$ are normed linear independent tangents at y_0. Thus we get an *initial triangle* $T = \{y_0, y_1, y_2\}$.

- For each new edge e of a triangle T construct an *imaginary triangle* $\hat{T}$ in the following way:
  - Compute the *nine parameter interpolant* of M with respect to the triangle T (see section 3).
  - Compute a steplength s taking into account the convergence behaviour of the Gauss Newton method for the points of the triangle T.
  - Consider the *local parameter plane* $\langle T \rangle$ spanned by T. Take the parameter on the outward normal on the midpoint of the edge e whose distance from e is equal to the stepsize s.
  - Compute the corresponding point $\hat{y}$ on the interpolating polynomial surface and take it as a guess for a new solution on M.
- Try to *realize* each imaginary triangle $\hat{T}$ in one of the following ways:
  - If $\hat{T}$ "overlaps" with an already computed triangle T, connect the vertex $\hat{y}$ of $\hat{T}$ with the corresponding point of T (see section 4).
  - Else, try to compute a new solution y by a Gauss Newton iteration $\hat{y} \overset{GN}{\longmapsto} y$.
- The algorithm stops if all imaginary triangles are realized (success) or some imaginary triangle cannot be realized (failure).

We see that the algorithm not only provides a triangulation of the surface but at the same time an approximation by a continuous piecewise cubic interpolating surface consisting of the nine parameter interpolants. This interpolating surface may also be used for the visualization of the implicit surface.

2 Affine invariant Gauss Newton techniques

If $y^0 = \hat{y}$ is some approximate solution of $f(y) = 0$, we use a Gauss Newton iteration $(k = 0, 1, \ldots)$

$$y^{k+1} = y^k + \Delta y^k, \quad \text{where} \quad Df(y^k)^+ \Delta y^k = -f(y^k) \tag{2.1}$$

is the *Gauss Newton correction* as a corrector scheme to compute a solution $y = \lim_{k\to\infty} y^k$ on M. The local convergence is guaranteed by the following theorem due to Deuflhard and Heindl [6].

THEOREM 1. *Let $f : D \subset \mathbf{R}^n \to \mathbf{R}^m$, $n > m$, be a differentiable mapping of an open convex set D in $\mathbf{R}^m$, such that all points $y \in D$ are regular. Assume the f satisfies for some $\omega > 0$ the affine invariant Lipschitz condition*

$$\|Df(w)^+(Df(v) - Df(u))\| \leq \omega\|v - u\|$$

for $u, v, w \in D$, $v - u \in \operatorname{im} Df(w)^+$. Let $y^0 \in D$ and suppose there is a constant $\alpha > 0$ such that

$$\begin{aligned} &i) \quad \|\Delta y^0\| = \|Df(y^0)^+ f(y^0)\| \leq \alpha, \\ &ii) \quad \bar{B}_r(y^0) = \{y \mid \|y - y^0\| \leq r\} \subset D, \\ &iii) \quad \frac{1}{2}\alpha\omega < 1. \end{aligned} \tag{2.2}$$

Then the Gauss Newton iterates y^k defined by (2.1) remain in $\bar{B}_r(y^0)$ and converge to a solution $y^* = \lim_{k\to\infty} y^k$ of $f(y) = 0$.

The convergence may be tested by the so-called *natural monotonicity test*

$$\theta_k := \frac{\|\bar{\Delta} y^{k+1}\|}{\|\Delta y^k\|} \leq \frac{1}{2}, \tag{2.3}$$

where $\bar{\Delta} y^{k+1}$ is the so-called *simplified Gauss Newton correction*

$$\bar{\Delta} y^{k+1} := -Df(y^k)^+ f(y^{k+1}). \tag{2.4}$$

If a direct solver is used, this may be easily computed using the decomposition of the Jacobian $Df(y^k)$.

The quotient θ_k plays a central role in the affine invariant steplength control mechanism used in the continuation codes ALCON [12] and SYMCON [10]. If we combine (for $k = 1$) the Gauss Newton method with the tangent continuation $\hat{y} = y + st(y)$, where $t(y)$ is a normed tangent vector at a known solution $y \in M$, the factor $\sqrt{\bar{\theta}/\theta_k}$, $\bar{\theta} := 0.25$, may be used to decrease the steplength s in case of a failure of the Gauss Newton iteration (*steplenth corrector*). On the other hand it also provides a *steplenth predictor* by possibly increasing the steplength if the Gauss Newton iteration converged. For details and a theoretical foundation based on the convergence theorem 1 see [12]. We will use this steplength control more or less heuristically in our two-dimensional continuation method.

3 BERNSTEIN-BÉZIER PATCHES AND THE NINE PARAMETER INTERPOLANT

Consider again the implicitly defined surface $M \subset \mathbf{R}^n$ and let $y_0, y_1, y_2 \in M$ be three affine independent points on M. We will call $T = \{y_0, y_1, y_2\}$ a *triangle on* M. In this section we look for a suitable polynomial interpolant for the data given by the points y_i and the corresponding tangent spaces $T_{y_i}M$ of M at y_i.

In order to define this bivariate Hermite interpolant, the so-called nine parameter interpolant (see e.g. Farin [8]) with a particular parametrization, we have to introduce some notions concerning triangular Bernstein-Bèzier patches. We will use the affine plane $\langle A \rangle := \langle y_0, y_1, y_2 \rangle$ spanned by the points y_i as the *local parameter plane* corresponding to the given triangle T. To define a polynomial on $\langle A \rangle$, we could easily use a linear coordinate system on $\langle A \rangle$, i.e. consider the affine plane $\langle A \rangle$ as a vector space with origin, say, y_0. For our purposes however, it is more convenient to use the barycentric coordinates $\lambda = (\lambda_0, \lambda_1, \lambda_2)$ of a point $y \in \langle A \rangle$ with respect to T defined by $y = \sum_{i=0}^{2} \lambda_i y_i$, where $\sum_{i=0}^{2} \lambda_i = 1$. This is an affine isomorphism

$$\mathbf{A}^2 \longrightarrow \langle A \rangle, \quad \lambda \longmapsto \sum_{i=0}^{2} \lambda_i y_i$$

of the standard affine plane $\mathbf{A}^2 := \{\lambda \in \mathbf{R}^3 \mid \sum_{i=0}^{2} \lambda_i = 1\}$ onto $\langle A \rangle$. The convex hull of T, which we denote by $[T] := \mathrm{co}(y_0, y_1, y_2)$, corresponds to the standard 2-simplex

$$\Sigma^2 := \{\lambda \in \mathbf{A}^2 \mid \lambda_i \geq 0 \text{ for all } i = 0, 1, 2\} .$$

Hence we will often identify $\langle T \rangle$ and $[T]$ with the standard plane $\mathbf{A}^2$ and the standard triangle Σ^2 respectively. A *polynomial of degree k on $\mathbf{A}^2$* (and thus on $\langle A \rangle$) now is a homogeneous polynomial of degree k in the barycentric coordinates.

A basis of the space $P^k(\mathbf{A}^2, \mathbf{R})$ of polynomials of degree k on $\mathbf{A}^2$ is therefore given by the homogeneous monomials λ^α, $|\alpha| = k$, where we use the standard multi index notation for $\alpha = (\alpha_0, \alpha_1, \alpha_2) \in \mathbf{N}^3$:

$$\lambda^\alpha = \lambda_0^{\alpha_0} \lambda_1^{\alpha_1} \lambda_2^{\alpha_2}, \quad |\alpha| = \alpha_0 + \alpha_1 + \alpha_2, \quad \alpha! = \alpha_0! \, \alpha_1! \, \alpha_2! .$$

For cubic polynomials, $k = 3$, we get for instance

$$\lambda_0^3, \ \lambda_1^3, \ \lambda_2^3, \ \lambda_0^2\lambda_1, \ \lambda_0^2\lambda_2, \ \lambda_0\lambda_1^2, \ \lambda_1^2\lambda_2, \ \lambda_0\lambda_2^2, \ \lambda_1\lambda_2^2, \ \lambda_0\lambda_1\lambda_2 .$$

An alternativ basis for $P^k(\mathbf{A}^2, \mathbf{R})$ are the *Bernstein polynomials* B^k_α, $|\alpha| = k$, defined by

$$B^k_\alpha(\lambda) := \frac{k!}{\alpha!}\lambda^\alpha \, .$$

They share with the univariate Berstein polynomials $B^k_i(\mu) = \binom{k}{i}\mu^i(1-\mu)^{k-i}$ almost all properties which make them the basis of choice in CAGD applications. Since they are the terms of the trinomial expansion of $1 = (\sum_{i=0}^2 \lambda_i)^k$, they form a *partition of unity*, i.e. $\sum_{|\alpha|=k} B^k_\alpha = 1$, and they are obviously non negativ on the simplex Σ^2 or equivalently on the triangle $[T]$. The coefficients b_α of a polynomial

$$p = \sum_{|\alpha|=k} b_\alpha B^k_\alpha \in P^k(\mathbf{A}^2, \mathbf{R}) \tag{3.1}$$

with respect to the Bernstein polynomials are called *Bézier coefficients* or *Bézier points* of p, a polynomial as in (3.1) is called *triangular Bézier patch.* The Bézier points have the nice geometric property that for $\lambda \in \Sigma^s$ the value $p(\lambda)$ lies in the convex hull $\mathrm{co}\{b_\alpha\}$ of the Bézier points, see figure 3. Of

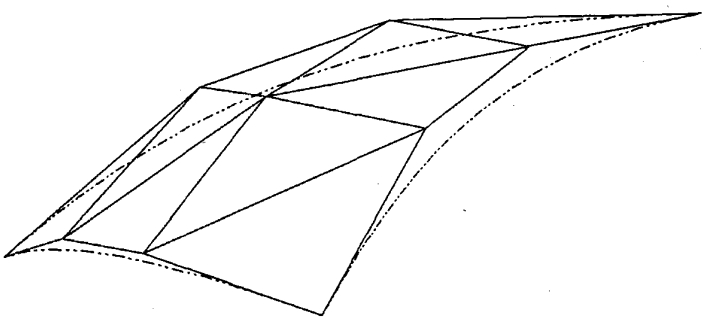

FIG. 1. A triangular Berstein-Bézier patch and its Bézier net

course these considerations remain valid if we consider the space $P^k(\mathbf{A}^2, \mathbf{R}^n)$ of polynomials of degree k with coefficients in $\mathbf{R}^n$, i.e. $p = \sum_{|\alpha|=k} b_\alpha B^k_\alpha$ with $b_\alpha \in \mathbf{R}^n$.

As in the univariate case, Casteljau's algorithm may be employed as the basic tool for the evaluation of the polynomial and its derivatives as well as for the approximation of the surface by successive subdivision.

We now first describe the standard nine parameter interpolant of a parametric sufficiently smooth surface $g : \mathbf{A}^2 \to \mathbf{R}^n$, $\lambda \mapsto g(\lambda)$. As usual let

$e_i \in \mathbf{A}^2$ for $i = 0, \ldots, 2$ be the vertices of the standard triangle Σ^2. We construct a cubic polynomial p on $\mathbf{A}^2$ that interpolates g and its first derivatives in the vertices e_i. Thus p has to satisfy the following nine conditions

$$\text{(3.2)} \quad \begin{aligned} &\text{i)} \quad g(e_i) = p(e_i) \quad \text{for } i = 0, \ldots, 2, \\ &\text{ii)} \quad D_{e_j - e_i} g(e_i) = D_{e_j - e_i} p(e_i) \quad \text{for } i, j = 0, \ldots, 2 \text{ and } i \neq j. \end{aligned}$$

The Bézier points of $p = \sum_{|\alpha|=3} b_\alpha B_\alpha^3$ are given by (see Farin [8])

$$\text{(3.3)} \quad \begin{aligned} &\text{i)} \quad b_{3e_i} = g(e_i) \quad \text{for } i = 0, \ldots, 2, \\ &\text{ii)} \quad b_{2e_i + e_j} = g(e_i) + \tfrac{1}{3} D_{e_j - e_i} g(e_i) \quad \text{for } i, j = 0, \ldots, 2 \text{ and } i \neq j, \\ &\text{iii)} \quad b_{1,1,1} = \tfrac{1}{4} \textstyle\sum_{i \neq j} b_{2e_i + e_j} - \tfrac{1}{6} \sum_i b_{3e_i}. \end{aligned}$$

The corresponding interpolation operator is of quadratic precision, i.e. quadratic surfaces $g \in P^2(\mathbf{A}^2, \mathbf{R}^n)$ will be reproduced.

Next we turn back to the implicitly defined surface $M = \{y \mid f(y) = 0\}$ and a triangle $T = \{y_0, y_1, y_2\}$ on M. We assume that there is a local coordinate system for M around T. More precisely there is a parametrization $g : U \subset \langle T \rangle \to \mathbf{R}^n$ of M, where $U \subset \langle T \rangle$ is an open neighbourhood of the triangle $[T]$ in $\langle T \rangle$, and an open neighbourhood $V \subset \mathbf{R}^n$ of $[T]$ in $\mathbf{R}^n$ such that

$$M \cap V = \{g(y) \mid y \in U\}.$$

Since the parametrization g is not uniquely determined by M, we cannot apply (3.3) directly. In order to construct a more or less canonical interpolating polynomial surface $p \in P^k(\langle T \rangle, \mathbf{R}^n)$, we require the directional derivative $D_{y_j - y_i} g(y_i)$ of g at the vertex y_i to be some scalar multiple of the normed orthogonal projection t_{ij} of the edge $y_j - y_i$ on the tangent space $T_{y_i} M = \ker Df(y_i)$ of M at y_i, i.e.

$$\text{(3.4)} \quad \begin{aligned} &\text{i)} \quad D_{y_j - y_i} g(y_i) = l_{ij} t_{ij}, \quad \text{where } l_{ij} \in \mathbf{R} \text{ and} \\ &\text{ii)} \quad t_{ij} = \text{orthogonal projection of } y_j - y_i \text{ on } \ker Df(y_i). \end{aligned}$$

A suitable heuristic choice for the scalar factors l_{ij} is $l_{ij} := 1.2 \cdot \|y_j - y_i\|$, see Farin [9], chapter 8. Using (3.3), we may now construct a cubic interpolating surface for M by

$$\text{(3.5)} \quad \begin{aligned} &\text{i)} \quad b_{3e_i} = y_i \quad \text{for } i = 0, \ldots, 2, \\ &\text{ii)} \quad b_{2e_i + e_j} = y_i + 0.4 \, \|y_j - y_i\| \, t_{ij} \quad \text{for } i, j = 0, \ldots, 2 \text{ and } i \neq j, \\ &\text{iii)} \quad b_{1,1,1} = \tfrac{1}{4} \textstyle\sum_{i \neq j} b_{2e_i + e_j} - \tfrac{1}{6} \sum_i b_{3e_i}. \end{aligned}$$

4 Overlaps and how to avoid them

On of the main difficulties of the two-dimensional continuation algorithm is the detection of overlaps of the successively constructed triangles and the way how to deal with them. This problem already exists in the one parameter case but is of less importance there. Most pathfollowing programs will run into an endless loop if they have to compute a curve as simple as the circle $S^1 = \{y \in \mathbf{R}^2 \mid \|y\|^2 - 1 = 0\}$. We have to answer the following question:

> "Under which circumstances should an imaginary triangle be connected to an already computed point?"

To answer this question, we think of the triangulation as a *locally plane* one, i.e. a triangulation of the Euclidian plane. Obviously we have to guarantee that this simple model is feasible. In order to achieve this, we restrict the angles $\sphericalangle(t_{ij}, t_{ji})$ between the normed orthogonal projections t_{ij} of an edge $\overline{y_i y_j}$ onto the tangent spaces $T_{y_i}M$ and $T_{y_j}M$, respectively. More precisely, we require these tangents to satisfy

$$|\langle t_{ij}, t_{ji}\rangle| \geq \alpha_{\min},$$

or equivalently

$$\sphericalangle(t_{ij}, t_{ji}) \leq \arccos(\alpha_{\min}),$$

where we choose $\alpha_{\min} := 0.8$, corresponding to an maximal angle of about $\arccos(\alpha_{\min}) \approx 36.8°$.

Now thinking of the triangulation of a plane, one criterion for the connection of triangles is the avoidance of overlaps. As a first rule, an imaginary triangle must be connected to an already known vertex y if the imaginary triangle and a real triangle, having y as a vertex, overlap. Thereby we may restrict ourselves to the *boundary vertices*, i.e. the vertices which belong to other imaginary triangles. Hence, in what follows, only these vertices, which normally form a small subset of all vertices, are to be taken into account. We distinguish three different kinds of overlaps:

- *close overlaps*: The imaginary triangle and a neighbouring real triangle overlap, see figure 2.
- *distant overlaps*: The imaginary triangle and a far, i.e. not neighbouring, real triangle overlap, see figure 3.
- *imaginary overlaps*: The imaginary triangle and another imaginary neighbouring triangle overlap, see figure 4.

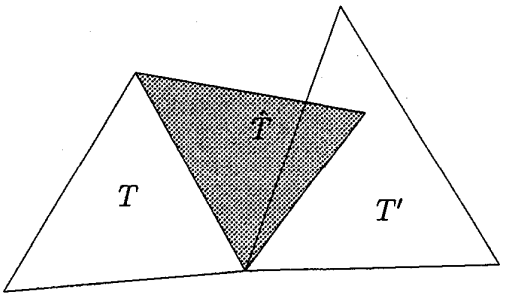

FIG. 2. Close overlap

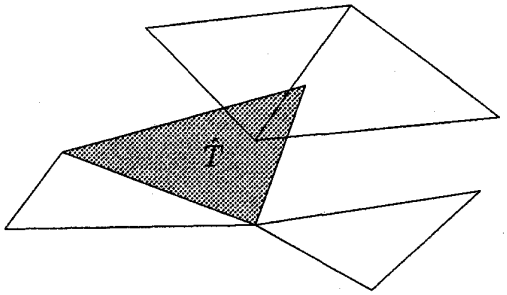

FIG. 3. Distant overlap

The easiest way to detect these situations is to use the geometrical properties of the barycentric coordinates $\lambda^T = (\lambda_0^T, \lambda_1^T, \lambda_2^T)$ with respect to a triangle $T = \{y_0, y_1, y_2\}$ (see figure 5). A point $y \in \langle T \rangle$ belongs to the triangle $[T]$ if and only if all barycentric coordinates $\lambda_i^T(y)$ are non negativ, i.e. $\lambda^T(y) \geq 0$ componentwise. The straight line $\overline{pq}$ between two points $p, q \in \langle T \rangle$ touches the triangle T if and only if one of the following conditions holds:

a) $\lambda^T(p) \geq 0$ or $\lambda^T(q) \geq 0$,

b) $\lambda_i^T(p) < 0$ for some $i \in \{0,1,2\}$ and $\lambda_1^{\tilde{T}}(q), \lambda_2^{\tilde{T}}(q) \geq 0$, where $\{i,j,k\} = \{0,1,2\}$ and $\tilde{T}$ is the triangle $\tilde{T} := \{p, y_j, y_k\}$.

Since two triangles overlap if and only if an edge of one of the triangles touches the other triangle, all kinds of overlaps can be detected by these means.

In view of our plane triangulation model we take for arbitrary points $y \in \mathbf{R}^n$, not necessarily on $\langle T \rangle$, the barycentric coordinates of the orthogonal

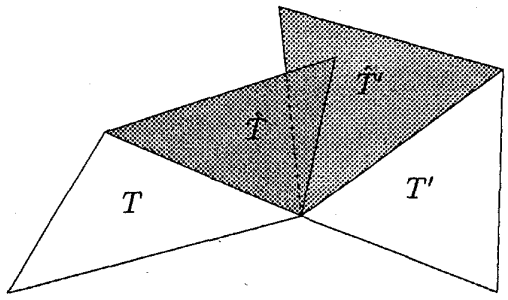

FIG. 4. Imaginary overlap

projection of y onto the triangle plane $\langle T \rangle$. Of course we have to ensure that this projection does not forget the local character of our model. For overlaps of neighbouring triangles there is nothing to worry about. For far overlaps we have to restrict the distance of the two triangles under investigation.

5 DETAILS OF IMPLEMENTATION

In this Section we want to fill in some gaps left in the rough description of the algorithm in Section 1.

Construction of imaginary triangles. To begin with, we will have a closer look onto the construction of an imaginary triangle $\hat{T}$. Consider the situation depicted in figure 6. We have a triangle T on M and want to form a model $\hat{T} = \{y_j, y_k, \hat{y}\}$ for a new triangle that fits to the edge $e = \{y_j, y_k\}$ of T. In Section 3 we constructed the nine parameter interpolant $p : \langle T \rangle \to \mathbf{R}^n$ corresponding to T, defined on the local parameter plane $\langle T \rangle$. Thus, to compute a guess $\hat{y}$ for the yet unknown third vertex, we have to choose a parameter $\tilde{y} \in \langle T \rangle$, then taking $\hat{y} = p(\tilde{y})$ on the interpolating surface. Let $t \in \langle T \rangle - y_0$ be the outward normal on the edge e in the parameter plane, $\langle t, y_k - y_j \rangle = 0$ and $\|t\| = 1$, and $\bar{y} := (y_j + y_k)/2$ the midpoint of e. We now choose the point

$$\tilde{y} := \bar{y} + st$$

on the outward normal at $\bar{y}$ whose distance from $\bar{y}$ is the prescribed steplength s. To determine s we consider the vertices y_j and y_k which have been computed by a Gauss Newton process using the steplenths s_j and s_k. The Gauss Newton iterations provide us with the quotients θ_j and θ_k of the norms of

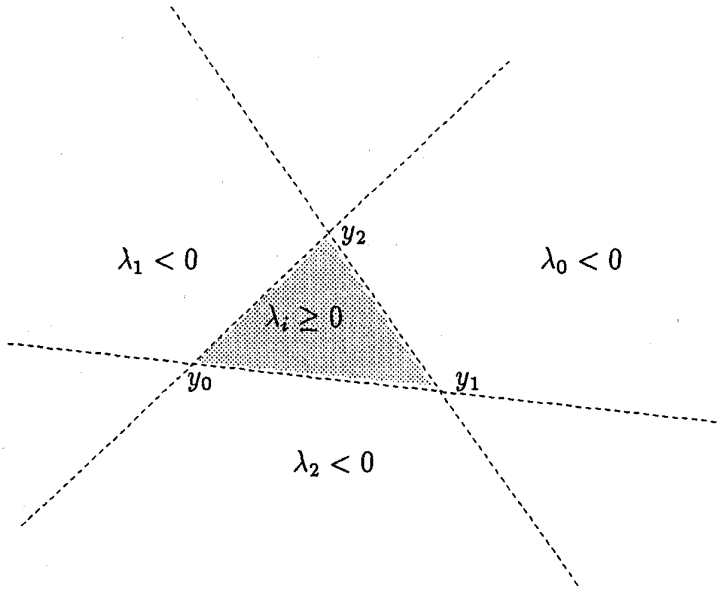

FIG. 5. Geometrical properties of the barycentric coordinates

the first simplified and ordinary Gauss Newton corrections. Since the nine parameter interpolant preserves the tangent planes at the vertices of T, it is feasible to use the factors $\sqrt{\bar{\theta}/\theta_j}$ and $\sqrt{\bar{\theta}/\theta_k}$, known for tangent continuation methods, to increase the steplengths s_j and s_k. To further simplify the steplength strategy (predictor) we now take

$$s := \min\left(\sqrt{\frac{\bar{\theta}}{\theta_j}}s_j, \sqrt{\frac{\bar{\theta}}{\theta_k}}s_k\right)$$

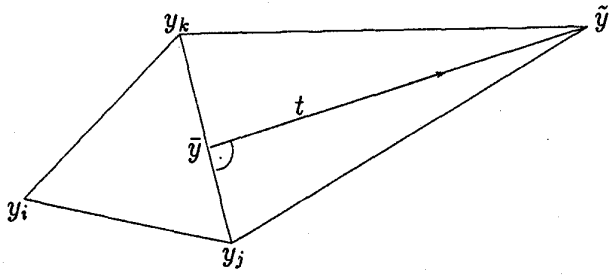

FIG. 6. Construction of an imaginary triangle.

as the new steplength. To compute the imaginary vertex $\hat{y} = p(\tilde{y})$ we use Casteljau's algorithm which gives us the Bézier net corresponding to the imaginary $\hat{T}$ as additional information. More precisely, let $\hat{y}_0 = y_j$, $\hat{y}_1 = y_k$ and $\hat{y}_2 = \hat{y}$ be the vertices of $\hat{T}$ and let S be the cubic interpolating surface defined (explicitly) by p. Then we get the Bézier points $\{\hat{b}_\alpha\}$, $|\alpha| = 3$, with respect to the vertices $\hat{y}_i$. In particular, we are given the vertices $\hat{b}_{3e_i} = \hat{y}_i$ and the tangent vectors $\hat{b}_{2e_i+e_j} - \hat{b}_{3e_i} \in T_{\hat{y}_i}S$. By $\hat{t}_{ij} \in T_{\hat{y}_i}S$ we denote the normed tangents

$$\hat{t}_{ij} := \frac{\hat{b}_{2e_i+e_j} - \hat{b}_{3e_i}}{\|\hat{b}_{2e_i+e_j} - \hat{b}_{3e_i}\|}.$$

In view of our bound for the angles $\sphericalangle(t_{ij}, t_{ji})$ of a triangle on M, we also require the "imaginary tangents" $\hat{t}_{ij}$ to satisfy

$$|\langle \hat{t}_{ij}, \hat{t}_{ji} \rangle| \geq \alpha_{\min}.$$

If this condition is violated, we reduce the steplength s before any further calculations (e.g. Gauss Newton iterations) are carried out.

In figure 7 we show the initial triangle and its three imaginary triangles. On the left hand side the cubic boundary curves given by the Bézier polygons along the edges are plotted. On the right hand side we see the corresponding Bézier nets which all describe the same surface S but with respect to the four different triangles.

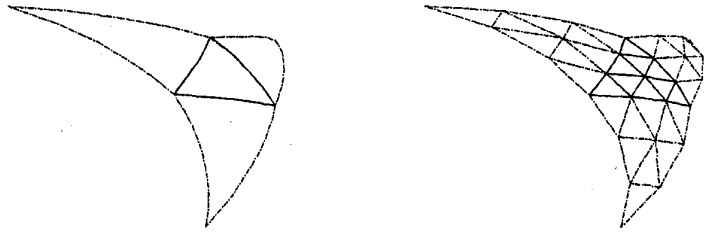

FIG. 7. Boundary curves and Bézier nets of the initial triangle and its imaginary triangles

Projections and barycentric coordinates. Next we describe how to compute the barycentric coordinates λ_i with respect to a triangle $T = \{y_0, y_1, y_2\}$. An orthonormal basis $\mathcal{B} = \{e_1, e_2\}$ of the vector space $\langle T \rangle - y_0$ is given by a single orthonormalization step

$$\begin{aligned} e_1 &:= \frac{y_1 - y_0}{\|y_1 - y_0\|}, \\ e_2 &:= \frac{v}{\|v\|}, \text{ where } v := y_2 - y_0 - \langle e_1, y_2 - y_0 \rangle e_1. \end{aligned}$$

During these calculations we save the constants

$$\alpha := \|y_1 - y_0\|,\ \beta := \langle e_1, y_2 - y_0\rangle,\ \text{and}\ \gamma := \|v\|.$$

They can be used to transform the cartesian coordinates x_i of a point $y = y_0 + \sum_{i=1}^{2} x_i e_i$ into the barycentric coordinates λ_i, where $y = \sum_{i=0}^{2} \lambda_i y_i$, and vice versa. Since $x_1 = \alpha\lambda_1 + \beta\lambda_2$ and $x_2 = \gamma\lambda_2$, we have

$$\lambda_2 = x_2/\gamma,\ \ \lambda_1 = (x_1 - \beta\lambda_2)/\alpha,\ \ \text{and}\ \ \lambda_0 = 1 - \lambda_1 - \lambda_2.$$

In addition, we may employ the orthonormal basis $\mathcal{B}$ to compute the orthogonal projection of a point $y \in \mathbf{R}^n$ on the triangle plane $\langle T\rangle$ by $y \mapsto y_0 + \sum_{i=1}^{2}\langle y - y_0, e_i\rangle e_i$, where $x_i = \langle y - y_0, e_i\rangle$ are the cartesian coordinates as above.

Connection of triangles. In order to develop a robust continuation argorithm, the conditions for overlaps of triangles as outlined in Section 4 have to be softened. Therefore we substitute each inequality $\lambda_i \leq 0$ for a barycentric coordinate λ_i by $\lambda_i \leq \rho$ and similarly $\lambda_i \geq 0$ by $\lambda_i \geq -\rho$, where $\rho > 0$ is some safety factor. In the present implementation we set $\rho := 0.3$.

Now let us consider the following situation of two neighbouring triangles T and T' and an imaginary triangle $\hat{T}$ at the edge e of T (see figure 8). Obviously $\hat{T}$ should be connected to T' to avoid a "thin" triangle correspond-

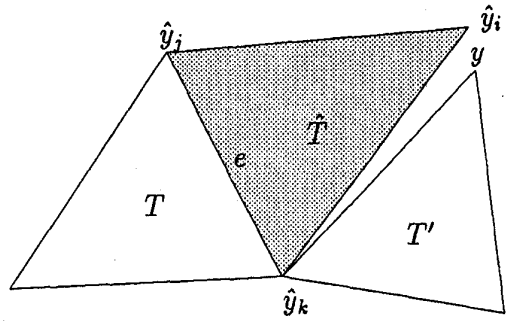

FIG. 8. Connection of two neighbouring triangles

ing to the points $\hat{y}_0, \hat{y}_i, y$. Thus we have to define under which circumstances an imaginary triangle $\hat{T}$ is *connectable* to a triangle T' on M. This time we use the triangle plane $\langle\hat{T}\rangle$ of the imaginary triangle and define a segment $S \subset \langle\hat{T}\rangle$ such that $\hat{T}$ is connectable to T' if the projection of y onto $\langle\hat{T}\rangle$ is

in S. For the segment S we choose

$$S := \left\{ y = \sum_{k=0}^{2} \lambda_k \hat{y}_k \;\middle|\; \lambda_0 \geq 0 \text{ and } \lambda_j \geq \beta(\lambda_i - 1) \text{ for } \{i,j\} = \{1,2\} \right\} .$$

where the constant β determines the width of the sector. The boundary of S intersects the line through $\hat{y}_0$ and $\hat{y}_1$ at $\lambda = (1+\beta, 0, -\beta)$, see figure 9. In the present implementation we set $\beta := 1.5$.

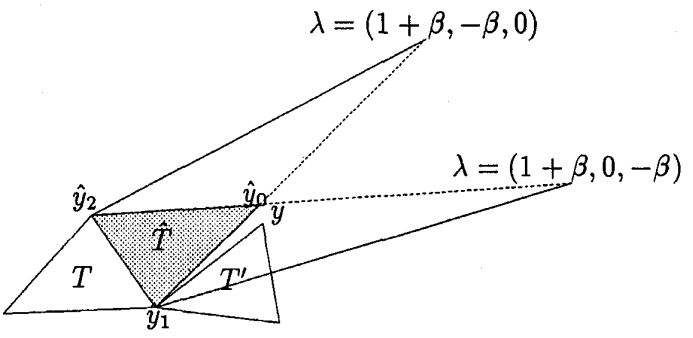

FIG. 9. Connection of two neighbouring triangles

6 NUMERICAL EXAMPLES

In this section we give some examples showing the two dimensional continuation method at work. Unfortunately we have to present our graphical results on a very low level since we had no advanced graphic package for three dimensional drawings at hand. So there are no rendered surfaces or even hidden lines removed. We hope the pictures are nevertheless able to visualize our results.

EXAMPLE 1. *Sphere.* As a first and very simple example consider the two dimensional sphere

$$S^2 = \{ y \in \mathbf{R}^3 \mid \|y\| = 1 \} = \{ y \in \mathbf{R}^3 \mid f(y) = \|y\|^2 - 1 = 0 \} .$$

In this example the stepsize is mainly determined by the restriction of the tangent angles because of the simplicity of the nonlinear equation.

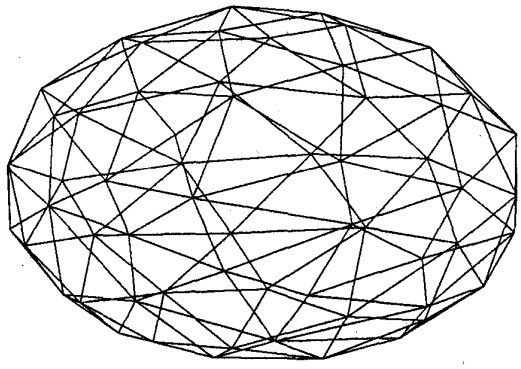

FIG. 10. Triangulation of the sphere

EXAMPLE 2. *Equipotential surface.* This is another example of a surface in three-dimensional space taken from Bloomenthal [5]. The defining function f is given by

$$f(y) := \frac{r_p^2}{\|y-p\|^2} + \frac{r_q^2}{\|y-q\|^2} - c = 0\,,$$

where $p, q \in \mathbf{R}^3$ and $r_p, r_q, c \in \mathbf{R}$. Here we have chosen $p = (0,0,0)$, $q = (0,2,0)$, $r_p = r_q = 1$, $c = 1.7$ and $\hat{y}_0 = (0,-0.8,0)$ as a first approximate solution. The stepsize reductions visible at the "saddle" of the surface are again forced by the geometrical difficulty.

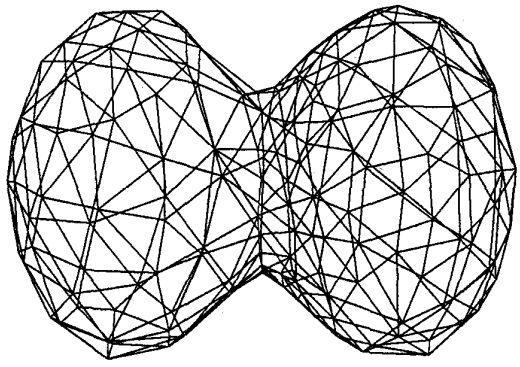

FIG. 11. Triangulation of the equipotential surface

EXAMPLE 3. *Cusp.* This surface, also known as the Whitney pleat, is defined by the cubic polynomial equation

$$f(y) = f(x, \lambda, \mu) = x^3 - \lambda x - \mu = 0 \, .$$

This examples shows that the algorithm is very easily extended to compute the solution set inside a prescribed compact box. For the solution points on some face of the box we fix a coordinate and use the Gauss-Newton iteration for the mapping restricted to this face. To produce Figure 12 we took $\hat{y}_0 = (0.1, 0.1, 0.1)$ (near the cusp point) as initial guess.

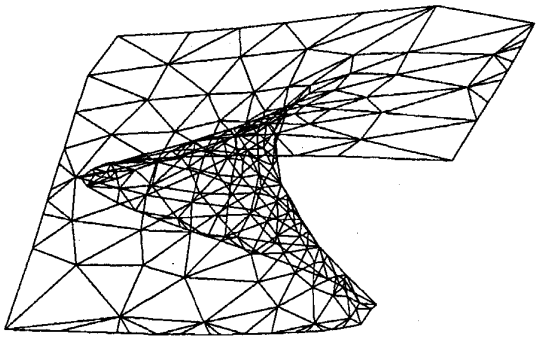

FIG. 12. Triangulation of the Whitney pleat (cusp)

EXAMPLE 4. *Torus.* Next we compute a triangulation for the torus define as an implicit surface by (see e.g. Allgower and Gnutzmann [2])

$$f(y) = (\|y\|^2 + R^2 - r^2)^2 - 4R^2(y_2^2 + y_3^2) = 0; ,$$

where $R, r \in \mathbf{R}$ are the major and minor radii. In Figure 13 we chose $R = 1$, $r = 0.4$ and $\hat{y}_0 = (-0.4, 1.0, 0.1)$ as initial guess.

EXAMPLE 5. *Continuous stirred tank reactor (CSTR).* To show that the algorithms is not confined to surfaces in three dimensional space, we consider the stationary solutions of a CSTR. According to [13] the steady states of a single first order reaction are given by

$$\begin{aligned} x_1 &= \mathrm{Da}(1 - x_1) \exp\left(\frac{x_2}{1 + x_2/\gamma}\right) \\ (1 + \beta)x_2 &= B\,\mathrm{Da}(1 - x_1) \exp\left(\frac{x_2}{1 + x_2/\gamma}\right) + \beta c \, , \end{aligned}$$

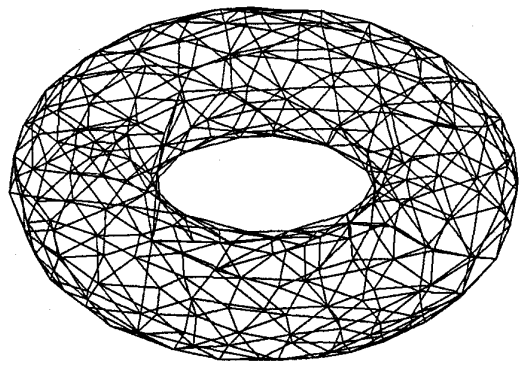

FIG. 13. Triangulation of the torus

where Da is the Damköhler number, x_1 the rescaled concentration and x_2, c, B, β, γ denote the dimensionless variables corresponding to temperature, cooling temperature, adiabatic temperature rise, heat transfer coefficient and activation energy, respectively. For simplicity we only consider the limit case $\gamma \to \infty$ and $c = 0$ (cf. [13]) leading to

$$\begin{aligned} x_1 &= \mathrm{Da}(1 - x_1)\exp(x_2) \\ (1+\beta)x_2 &= B\,\mathrm{Da}(1 - x_1)\exp(x_2)\,. \end{aligned}$$

Moreover we let β be constant and end up with a system of two nonlinear equations in the variables x_1, x_2, Da and B.

$$\begin{aligned} f_1(x_1, x_2, Da, B) &= -x_1 + \mathrm{Da}(1 - x_1)\exp(x_2) \\ f_2(x_1, x_2, Da, B) &= -(1+\beta)x_2 + B\,\mathrm{Da}(1 - x_1)\exp(x_2)\,. \end{aligned}$$

(Of course this system can easily be reduced to a single equation using the linear relationship $x_2 = Bx_2/(1+\beta)$, but we take it as it is.) The resulting surface is shown in Figure 14 where we chose $\beta = 0.5$ and $\hat{y}_0 = (0.1, 0.1, 0.1, 5)$ as initial guess.

Table I contains the numbers of vertices, edges and triangles computed by our method for the given examples. The interested reader may check the Euler characteristics to convince himself that there are no double coverings.

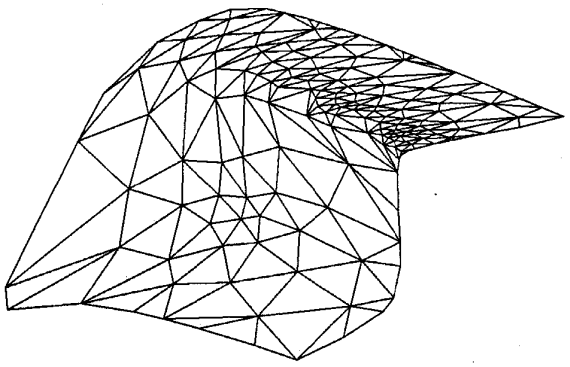

FIG. 14. Steady solutions of the CSTR, x_1 versus B and Da

example	points	edges	triangles
sphere	60	174	116
blobby	153	453	302
cusp	206	555	350
torus	273	819	546
cstr	166	447	282

TABLE I. Performance of the algorithm

CONCLUSION

We have developed a two-dimensional adaptive continuation algorithm generalizing the well established ideas for implicitly defined curves to the two-dimensional case. We have shown its reliability by means of a few small but instructive examples that in particular include the main geometrical difficulties. This is, of course, only a first step. Next we will have to apply the method to larger problems of real life applications that we are really interested in.

In addition, there are several theoretical problems left for further investigation. The approximation properties of the nine parameter interpolant in the non-parametrized case are not completely understood. In connection with the affine invariant convergence results for the Gauss-Newton method this will be the key for a less heuristical steplength control. We will cope with these questions in more detail in a forthcoming paper.

REFERÈNCES

[1] E. L. Allgower and K. Georg. *Numerical Continuation Methods.* Springer-Verlag, Berlin, Heidelberg, New York, 1990.

[2] E. L. Allgower and S. Gnutzmann. An algorithm for piecewise linear approximation of implicitly defined two-dimensional surfaces. *SIAM J. Numer. Anal.*, 24:452–469, 1987.

[3] E. L. Allgower and S. Gnutzmann. Simplicial pivoting for mesh generation of implicitly defined surfaces. *CAGD*, 8:305–325, 1991.

[4] E. L. Allgower and P. H. Schmidt. An algorithm for piecewise-linear approximation of an implicitly defined manifold. *SIAM J. Numer. Anal.*, 22:322–346, 1985.

[5] J. Bloomenthal. Polygonization of implicit surfaces. *CAGD*, 5:341–355, 1988.

[6] P. Deuflhard and G. Heindl. Affine invariant convergence theorems for newton's method and extensions to related methods. *SIAM J. Numer. Anal.*, 16:1–10, 1979.

[7] E. J. Doedel. AUTO: Software for continuation and bifurcation problems in ordinary differential equations. Technical report, California Institute of Technology, Pasadena, 1986.

[8] G. Farin. Triangular Berstein-Bézier patches. *Computer Aided Geometric Design*, 3:83–127, 1986.

[9] G. Farin. *Curves and Surfaces for Computer Aided Geometric Design: A Practical Guide.* Academic Press, New York, 1988.

[10] K. Gatermann and A. Hohmann. Symbolic exploitation of symmetry in numerical pathfollowing. Preprint SC 90–11, Konrad-Zuse-Zentrum, Berlin, 1990.

[11] H. B. Keller. Numerical solution of bifurcation and nonlinear eigenvalue problems. In P. H. Rabinowitz, editor, *Application of Bifurcation Theory*, pages 359–384. Academic Press, New York, London, 1977.

[12] P. Deuflhard, B. Fiedler, P. Kunkel. Efficient numerical pathfollowing beyond critical points. *SIAM J. Numer. Anal.*, 18:949–987, 1987.

[13] A. Uppal, W. H. Ray, A. B. Poore. On the dynamic behavior of continuous stirred tank reaktors. *Chem. Engng. Sci.*, 29:967–985, 1974.

[14] W. C. Rheinboldt. *Numerical analysis of parametrized nonlinear equations.* John Wiley and Sons, New York, 1986.

[15] W. C. Rheinboldt. On the computation of multi-dimensional solution manifolds of parametrized equations. Tech. Report ICMA-86-102, University Pittsburgh, 1986.

[16] R. Seydel. *From equilibrium to chaos. Practical bifurcation and stability analysis.* Elsevier, New York, 1988.

Veröffentlichungen des Konrad-Zuse-Zentrum für Informationstechnik Berlin
Preprints Dezember 1991

SC 90-1. M. Wulkow; P. Deuflhard. *Towards an Efficient Computational Treatment of Heterogeneous Polymer Reactions.*
SC 90-2. P. Deuflhard. *Global Inexact Newton Methods for Very Large Scale Nonlinear Problems.*
SC 90-3. K. Gatermann. *Symbolic solution of polynomial equation systems with symmetry.*
SC 90-4. F. A. Bornemann. *An Adaptive Multilevel Approach to Parabolic Equations I. General Theory & 1D-Implementation.*
SC 90-5. P. Deuflhard; R. Freund; A. Walter. *Fast Secant Methods for the Iterative Solution of Large Nonsymmetric Linear Systems.*
SC 90-6. D. Wang. *On Symplectic Difference Schemes for Hamiltonian Systems.*
SC 90-7. P. Deuflhard; U. Nowak; M. Wulkow. *Recent Developments in Chemical Computing.*
SC 90-8. C. Chevalier; H. Melenk; J. Warnatz. *Automatic Generation of Reaction Mechanisms for Description of Oxidation of Higher Hydrocarbons.*
SC 90-9. P. Deuflhard; F. A. Potra. *Asymptotic Mesh Independence of Newton-Galerkin Methods via a Refined Mysovskii Theorem.*
SC 90-10. R. Kornhuber; R. Roitzsch. *Self Adaptive FEM Simulation of Reverse Biased pn-Junctions.*
SC 90-11. K. Gatermann; A. Hohmann. *Symbolic Exploitation of Symmetry in Numerical Path-following.*
SC 90-12. A. Walter. *Improvement of Incomplete Factorizations by a Sparse Secant Method.*
SC 90-13. F. A. Bornemann. *An Adaptive Multilevel Approach to Parabolic Equations II.*
SC 90-14. J. Ackermann; M. Wulkow. *MACRON - A Program Package for Macromalecular Reaction Kinetics.*
SC 90-15. M. Wulkow; J. Ackermann. *Numerical Treatment of Polyreactions - Recent Developments.*
SC 90-16. H. C. Hege; H. Stüben. *Vectorization and Parallelization of Irregular Problems via Graph coloring.*
SC 90-17. D. Wang. *Symplectic Difference Schemes for Perturbed Hamiltonian Systems.*
SC 90-18. H.Caprasse; J. Demaret; K. Gatermann; H. Melenk. *Power-Law Type Solutions of Fourth-Order Gravity for Multidimensional Bianchi I Universes.*
SC 90-20. A. Walter. *Sparse Secant Methods for the Iterative Solution of Large Nonsymmetric Linear Systems.*

SC 91-1. F. A. Bornemann. *An Adaptive Multilevel Approach to Parabolic Equations III.*
SC 91-2. R. Kornhuber; R. Roitzsch. *Self Adaptive Computation of the Breakdown Voltage of Planar pn-Junctions with Multistep Field Plates.*
SC 91-3. A. Griewank. *Sequential Evaluation of Adjoints and Higher Derivative Vectors by Overloading and Reverse Accumulation.*
SC 91-4. P. Deuflhard; F. Potra. *Parameter Space Geometry and Convergence of Gauss-Newton Techniques.*
SC 91-5. B. Fiedler; J. Scheurle. *Discretization of Homoclinic Orbits, Rapid Forcing and "Invisible" Chaos.*
SC 91-6. R. H. W. Hoppe; R. Kornhuber. *Multilevel Preconditioned CG-Iterations for Variational Inequalities.*
SC 91-7. J. Lang; A. Walter. *An Adaptive Discontinuous Finite Element Method for the Transport Equation.*
SC 91-8. K. Gatermann; A. Hohmann. *Hexagonal Lattice Dome - Illustration of a Nontrivial Bifurcation Problem.*
SC 91-9. F. A. Bornemann. *A Sharpened Condition Number Estimate for the BPX Preconditioner of Elliptic Finite Element Problems on Highly Nonuniform Triangulations.*
SC 91-10. G. M. Ziegler. *Higher Bruhat Orders and Cyclic Hyperplane Arrangements.*
SC 91-11. B. Sturmfels; G. M. Ziegler. *Extension Spaces of Oriented Matriods.*
SC 91-12. F. Schmidt. *An Adaptive Approach to the Numerical Solution of Fresnel's Wave Equation.*
SC 91-13. R. Schöpf; P. Deuflhard. *OCCAL: A mixed symbolic-numeric Optimal Control CALculator.*
SC 91-14. G. M. Ziegler. *On the Difference Between Real and Complex Arrangements.*
SC 91-15. G. M. Ziegler; R. T. Zivaljevic. *Homotopy Types of Subspace Arrangements via Diagrams of Spaces.*
SC 91-16. R. H. W. Hoppe; R. Kornhuber. *Adaptive Multilevel - Methods for Obstacle Problems.*
SC 91-17. M. Wulkow. *Adaptive Treatment of Polyreactions in Weighted Sequence Spaces.*
SC 91-18. J. Ackermann; M. Wulkow. *The Treatment of Macromolecular Processes with Chain-Length-Dependent Reaction Coefficients - An Example from Soot Formation.*
SC 91-19. C. D. Godsil; M. Grötschel; D. J. A. Welsh. *Combinatorics in Statistical Physics.*
SC 91-20. A. Hohmann. *A Continuation Method for Implicitly Defined Surfaces.*

Veröffentlichungen des Konrad-Zuse-Zentrum für Informationstechnik Berlin
Technical Reports **Dezember 1991**

TR 90-1. K. Gatermann. *Gruppentheoretische Konstruktion von symmetrischen Kubaturformeln.*

TR 90-2. G. Maierhöfer; G. Skorobohatyj. *Implementierung von parallelen Versionen der Gleichungslöser EULEX und EULSIM auf Transputern.*

TR 90-3. *CRAY-Handbuch. Einführung in die Benutzung der CRAY X-MP unter UNICOS 5.1*

TR 90-4. H.-C. Hege. *Datenabhängigkeitsanalyse und Programmtransformationen auf CRAY-Rechnern mit dem Fortran-Präprozessor* ***fpp.***

TR 90-5. M. Grammel; G. Maierhöfer; G. Skorobohatij. *Trapex in POOL; Implementierung eines numerischen Algorithmus in einer parallelen objektorientierten Sprache.*

TR 90-6. P. Deuflhard; A. Hohmann. *Einführung in die Numerische Mathematik.*

TR 90-7. P. Deuflhard. *Zuses Werk weiterdenken. (Vortrag)*

TR 90-8. M. Wulkow. *Numerical Treatment of Countable Systems of Ordinary Differential Equations.*

TR 90-9. R. Roitzsch; R. Kornhuber. *BOXES - a Program to Generate Triangulations from a Rectangular Domain Description.*

TR 90-11. U. Nowak; L. Weimann. *GIANT - A Software Package for the Numerical Solution of Very Large Systems of Highly Nonlinear Equations.*

TR 90-13. W. K. Giloi. *Konrad Zuses Plankalkül als Vorläufer moderner Programmier-modelle. (Vortrag)*

TR 91-1. F. Bornemann; B. Erdmann; R. Roitzsch. *KASKADE - Numerical Experiments.*

TR 91-2. J. Lügger; W. Dalitz. *Verteilung mathematischer Software mittels elektronischer Netze: Die elektronische Softwarebibliothek eLib.*

TR 91-3. S. W. C. Noelle. *On the Limits of Operator Splitting: Numerical Experiments for the Complex Burgers Equation.*

TR 91-4. J. Lang. *An Adaptive Finite Element Method for Convection-Diffusion Problems by Interpolation Techniques.*

TR 91-5. J. Gottschewski. *Supercomputing During the German Reunification.*

TR 91-6. K. Schöffel. *Computational Chemistry Software for CRAY X-MP/24 at Konrad-Zuse-Zentrum für Informationtstechnik Berlin.*

TR 91-7. F. A. Bornemann. *An Adaptive Multilevel Approach to Parabolic Equations in Two Space Dimensions.*

TR 91-8. H. Gajewski; P. Deuflhard; P. A. Markowich (eds.). *Tagung NUMSIM '91 _5.-8. Mai 1991_ Collected Abstracts and Papers.*

TR 91-9. P. Deuflhard; U. Nowak; U. Pöhle; B. Ch. Schmidt; J. Weyer. *Die Ausbreitung von HIV/AIDS in Ballungsgebieten.*

TR 91-10. U. Nowak; L. Weimann. *A Family of Newton Codes for Systems of Highly Nonlinear Equations.*